



Dynamic spatiotemporal graph network for traffic accident risk prediction

Pengcheng Zhang, Wen Yi, Yongze Song, Penggao Yan, Peng Wu, Ammar Shemery, Keith Hampson & Albert P. C. Chan

To cite this article: Pengcheng Zhang, Wen Yi, Yongze Song, Penggao Yan, Peng Wu, Ammar Shemery, Keith Hampson & Albert P. C. Chan (2025) Dynamic spatiotemporal graph network for traffic accident risk prediction, GIScience & Remote Sensing, 62:1, 2514330, DOI: [10.1080/15481603.2025.2514330](https://doi.org/10.1080/15481603.2025.2514330)

To link to this article: <https://doi.org/10.1080/15481603.2025.2514330>



© 2025 The Author(s). Published by Informa UK Limited, trading as Taylor & Francis Group.



Published online: 14 Jun 2025.



Submit your article to this journal [↗](#)



Article views: 2750



View related articles [↗](#)



View Crossmark data [↗](#)



Citing articles: 1 View citing articles [↗](#)

Dynamic spatiotemporal graph network for traffic accident risk prediction

Pengcheng Zhang^a, Wen Yi^a, Yongze Song^b, Penggao Yan^c, Peng Wu^b, Ammar Shemery^d, Keith Hampson^d and Albert P. C. Chan^a

^aDepartment of Building and Real Estate, The Hong Kong Polytechnic University, Hong Kong, China; ^bSchool of Design and the Built Environment, Curtin University, Perth, Australia; ^cDepartment of Aeronautical and Aviation Engineering, Faculty of Engineering, The Hong Kong Polytechnic University, Hung Hom, Hong Kong, China; ^dSustainable Built Environment National Research Centre, Curtin University, Perth, Australia

ABSTRACT

Traffic accidents remain major public safety concerns, often causing severe injuries, deaths, and economic costs, especially in rapidly urbanizing areas. Accurate traffic accident risk prediction is crucial for developing effective strategies to reduce accidents and enhance urban mobility. However, predicting traffic accident risks is challenging due to the relationships among factors such as weather, traffic conditions, and road characteristics, along with capturing spatial correlations of traffic accidents across different time scales. To address these challenges, we propose the dynamic spatial-temporal accident risk network (DSTAR-Net). Our model uses channel-wise convolutional neural networks to detect spatial accident patterns across weekly, daily, and hourly time scales with automatic weight learning, simultaneously employing graph convolutional networks to process road network features, population feature while integrating external data like weather and dates. The dynamic learning of spatial correlations, combined with the integration of road characteristics and contextual variables, significantly enhances the accuracy of traffic accident predictions. Experiments in Perth show the DSTAR-Net outperforms state-of-the-art models with RMSE 24.901, Recall 21.59%, and MAP 0.0721. Notably, the weights learned by our model indicate that hourly patterns have the highest weight at 0.390, while weekly trends carry the lowest weight at 0.255, suggesting that recent traffic conditions have the most significant influence on accident risks. This study provides a foundational framework for predicting traffic accident risks, aiding urban planners and policymakers in enhancing road safety and traffic management in cities.

ARTICLE HISTORY

Received 22 December 2024
Accepted 28 May 2025

KEYWORDS

Traffic accidents prediction;
spatial-temporal analysis;
urban computing; intelligent
transportation

1. Introduction

Traffic accidents pose significant risks, causing severe consequences for individuals and society (Bucsuházy et al. 2020; Chand, Jayesh, and Bhasi 2021; Mohammed et al. 2019). These incidents lead to numerous injuries and fatalities, with thousands of people losing their lives annually due to traffic-related incidents (Ahmed et al. 2023). Moreover, these accidents cause profound physical and emotional distress for victims and their families while also leading to a tragic loss of human capital for society (Anjuman et al. 2020). The economic impact of traffic accidents is substantial, with major costs from medical care, property damage, legal processes, and insurance claims that burden individuals and healthcare systems (Bougna, Hundal, and Taniform 2022). Accidents frequently result in traffic congestion, impeding the movement of goods and services and adversely impacting businesses and the broader

economy (Zheng et al. 2020). The complex effects underscore the necessity for efficient traffic accident risk prediction and management solutions.

Given the profound implications for public safety and economic costs, accurate prediction of traffic accidents is essential for effective urban planning and targeted interventions that can significantly reduce collision risks (Gutierrez-Osorio and Pedraza 2020). Traffic accident prediction primarily involves utilizing historical accident data, environmental variables, and road-related information to identify patterns of accident occurrence and predict their locations in future timeframes. In contrast, traffic accident risk prediction assesses the likelihood and severity of potential accidents, enabling a more comprehensive understanding of safety challenges (B. Wang et al. 2021). Accurate predictions of accident risks necessitate evaluating the probability of accidents occurring in specific areas or road segments within a given period (Brühwiler et al. 2022). Authorities can allocate resources, implement targeted safety measures,

CONTACT Wen Yi  wen.yi@polyu.edu.hk; Yongze Song  yongze.song@curtin.edu.au

© 2025 The Author(s). Published by Informa UK Limited, trading as Taylor & Francis Group.

This is an Open Access article distributed under the terms of the Creative Commons Attribution License (<http://creativecommons.org/licenses/by/4.0/>), which permits unrestricted use, distribution, and reproduction in any medium, provided the original work is properly cited. The terms on which this article has been published allow the posting of the Accepted Manuscript in a repository by the author(s) or with their consent.

and raise awareness to reduce the occurrence and severity of accidents by identifying high-risk areas (Alkaabi 2023; Zhang, Li, and Song 2024). Accurate risk prediction aids in making proactive decisions and developing effective traffic management strategies (Chen et al. 2021).

The methods for predicting traffic accidents can be categorized into three main approaches: traditional statistical methods, machine learning methods, and deep learning methods. Traditional statistical methods are widely used, applying regression analysis, Bayesian networks, and time series forecasting techniques (Tang et al. 2020). These approaches analyze historical accident data to identify patterns and correlations with various influencing factors, including road characteristics, weather conditions, and traffic volumes (Abdulhafedh 2017; Chen, Chen, and Ma 2016). For example, crash prediction models (CPMs) estimate crash frequency by considering traffic flow and road design elements, which aids in identifying hazardous road sections (Ambros et al. 2018; Hossain et al. 2019). However, these methods struggle with the complexities of traffic data due to their reliance on linear assumptions, which may need to be more robust to capture the nonlinear relationships and interactions present in accident data (Mannering 2018). Furthermore, traditional methods frequently overlook spatial and temporal dependencies, limiting their predictive accuracy, particularly in dynamic urban environments.

To overcome traditional methods' limitations, machine learning has become a powerful tool with better flexibility for modeling complex data relationships (Zhou et al. 2017). Techniques such as decision trees, support vector machines, and ensemble methods have been applied to traffic accident prediction, enabling researchers to handle larger datasets and incorporate more variables (Jamal et al. 2021). These methods effectively handle nonlinearities and interactions among features, which traditional methods often overlook (Ali, Hussain, and Haque 2024). However, many machine learning models need to inherently consider the spatial relationships present in traffic data, which can lead to suboptimal predictions in urban settings (Lana et al. 2018).

Deep learning advances have significantly improved traffic accident prediction using advanced models. Core architectures, such as convolutional neural networks (CNNs) and long short-term memory (LSTM) networks, have proven effective in capturing complex spatial and temporal patterns (Graves and Graves 2012; O'Shea 2015; Shi et al. 2024). Chen et al. presented a stacked denoise convolutional autoencoder that incorporated spatial dependencies in traffic incidents through stacked CNNs to improve risk prediction by focusing on spatial

relationships (Chen et al. 2018). Moosavi et al. utilized LSTMs for nationwide risk prediction, demonstrating their capability to forecast risks at 15-minute intervals (Moosavi et al. 2019). Though CNNs excel spatially, they often struggle to model dynamic temporal changes. To address this, Ren et al. used LSTM to capture temporal correlations better, enabling predictions of traffic risks over time (Ren et al. 2018). Their work marked a significant step in incorporating temporal and spatial factors into deep learning urban traffic risk assessment frameworks.

Recent research highlights the complementary strengths of CNN and GCN in accident prediction. Wang et al. developed GSNet, where CNNs extract multi-scale patterns from accident heatmaps while GCNs model road networks via predefined adjacency matrices (Wang et al. 2021). However, their spatial features remain fixed, and they cannot adapt to traffic changes. Zhou et al. improved this in RiskOracle, using 3D-CNN for spatiotemporal patterns with hierarchical GCN processing road segments as dynamic nodes (Zhou, Wang, Xie, Chen, and Liu 2020). However, this method relies on the same fixed weight settings across all model components. Zhou et al. created RiskSeq, a GCN framework with multi-scale aggregation predicting sparse accidents across spatiotemporal scales, using regional proximity and temporal differences to model traffic changes (Zhou, Wang, Xie, Chen, and Zhu 2022). Their tests show GCN provides 68% accuracy gains for structural risks, but the CNN part misses the multi-temporal analysis needed for varying accident densities.

Despite advancements in traffic risk prediction, several significant challenges remain. One major issue is capturing the spatial correlations of traffic accidents across different time scales. Another challenge is integrating multisource data, which encompasses external features such as weather conditions and structural characteristics of roads. These gaps limit prediction accuracy, demanding a comprehensive framework that effectively fuses diverse data to boost prediction power (Shaik, Islam, and Hossain 2021).

Our proposed approach introduces the dynamic spatial-temporal accident risk network (DSTAR-Net) to address these challenges. One key aspect of our framework is its ability to capture spatial and semantic correlations across different time scales, as illustrated in Figure 1. Regions 1 and 2 are spatially adjacent, indicating an improved likelihood of traffic accidents due to their proximity. In contrast, regions 1 and 3 exhibit semantic correlation, as they share similar infrastructural features, making them equally prone to accidents. This distinction allows our model to effectively integrate spatial and semantic information to predict traffic accident

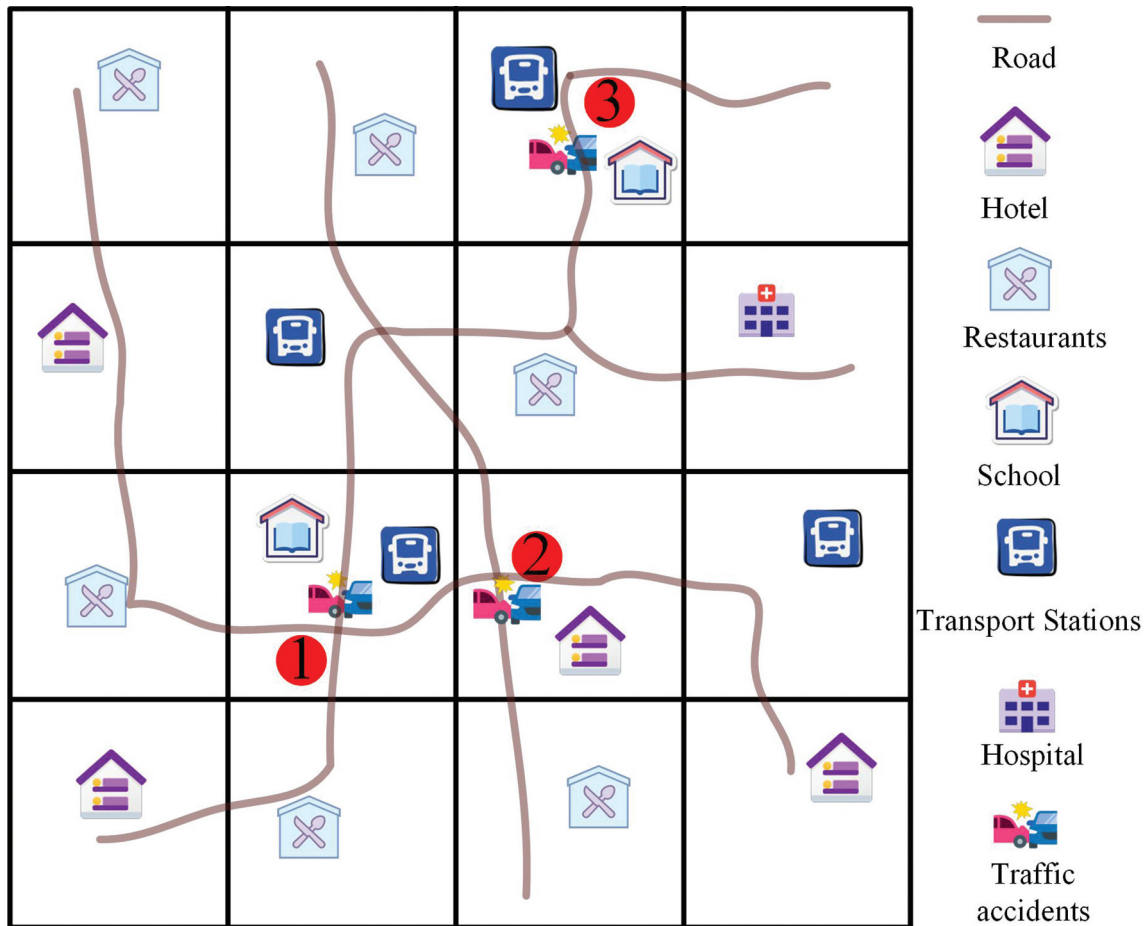


Figure 1. An example of using geographical and semantic spatial-temporal correlations to predict traffic accident risks.

risks. Our model uses channel-wise CNNs to learn local geographic patterns across different time periods, working with GCN to learn global road feature relationships. This design enables the dynamic adjustment of weights for each temporal module, enhancing the model's capability to extract relevant spatial and temporal information. Furthermore, we integrate contextual factors such as weather conditions, weekends, and holidays, thereby improving the accuracy of our predictions and addressing the challenge of multi-source data integration.

In summary, our contributions include: (1) the introduction of DSTAR-Net, a novel framework that enhances traffic accident risk prediction by modeling data across multiple temporal dimensions; (2) the use of channel-wise convolutional neural network (CNN) blocks to capture local geographic dependencies, complemented by a graph convolutional network (GCN) that learns global semantic relationships, integrating diverse data sources to improve risk assessment accuracy; and (3) experiments conducted with data from Perth, Western Australia, demonstrating that our model outperforms state-of-the-art methods in prediction accuracy.

The study consists of six sections. The first section introduces the research context and objectives. In the second section, the geographical context and datasets used are described. The third section discusses the methodologies applied in the research. Following that, the fourth section presents the experiments and their results. The fifth section interprets these findings in a detailed discussion. Finally, the sixth section wraps up the study by summarizing the findings and proposing areas for future research.

2. Study area and data

This study utilizes traffic accident data from the Perth Metropolitan region in Western Australia, the capital and fourth-most populous city in Australia, with a metropolitan population of over 2 million.

Perth's transportation network features an extensive road, suburban rail, and growing public bus systems. The city heavily relies on private vehicle usage, resulting in a high rate of car ownership among residents. This dependence has led to various challenges related to traffic congestion and road safety, which the region has been actively addressing in recent years.

The data used in this analysis is sourced from the Western Australian government and covers traffic accidents from 1 January 2018, to 31 December 2022 (Roads Western Australia 2024), comprising 109,670 traffic accidents, including 260 that resulted in fatalities. Table 1 provides a detailed overview of the statistics of traffic accident severity in Perth during this period.

Although our experiments utilized the complete five-year dataset, we select a subset to more clearly show the temporal and spatial trends. We first present the spatial distribution of traffic accident severity and other traffic-related factors. Figure 2a shows the spatial distribution of traffic accident severity in Perth from 2018.1.1 to 2022.12.31. Most traffic accidents are concentrated in

densely populated urban centers, while incidents are sparse in the outskirts. This pattern highlights the spatial distribution of traffic accidents, indicating that higher traffic volumes and more frequent interactions among vehicles in urban areas contribute to increased accident rates.

Figure 2b presents the spatial distribution of traffic speed limits in Perth, showing that roads with a speed limit of 50 km/h are the most prevalent, accounting for 89.55% of the total road network, with detailed statistics in Table 2. Meanwhile, Figure 2c displays the spatial distribution of points of interest (POIs) in Perth, where transport stations constitute approximately half of all identified POIs, highlighting the significance of these locations in influencing traffic patterns and accident

Table 1. Statistics of traffic accident severity in the Perth from 2018.1.1 to 2022.12.31.

Traffic accident severity	Description	Number	Proportion
Fatal	A fatal accident is a collision that results in the death of one or more individuals	259	0.27%
Hospital	A hospital accident involves injuries that require hospitalization but do not result in fatalities	4480	4.08%
Medical	A medical accident refers to injuries that require medical attention but do not necessitate hospitalization	14784	13.47%
PDO major	A PDO major accident involves significant property damage without any injuries or fatalities	58729	53.54%
PDO minor	A PDO Minor accident refers to incidents causing minimal property damage with no injuries or fatalities	31418	28.64%

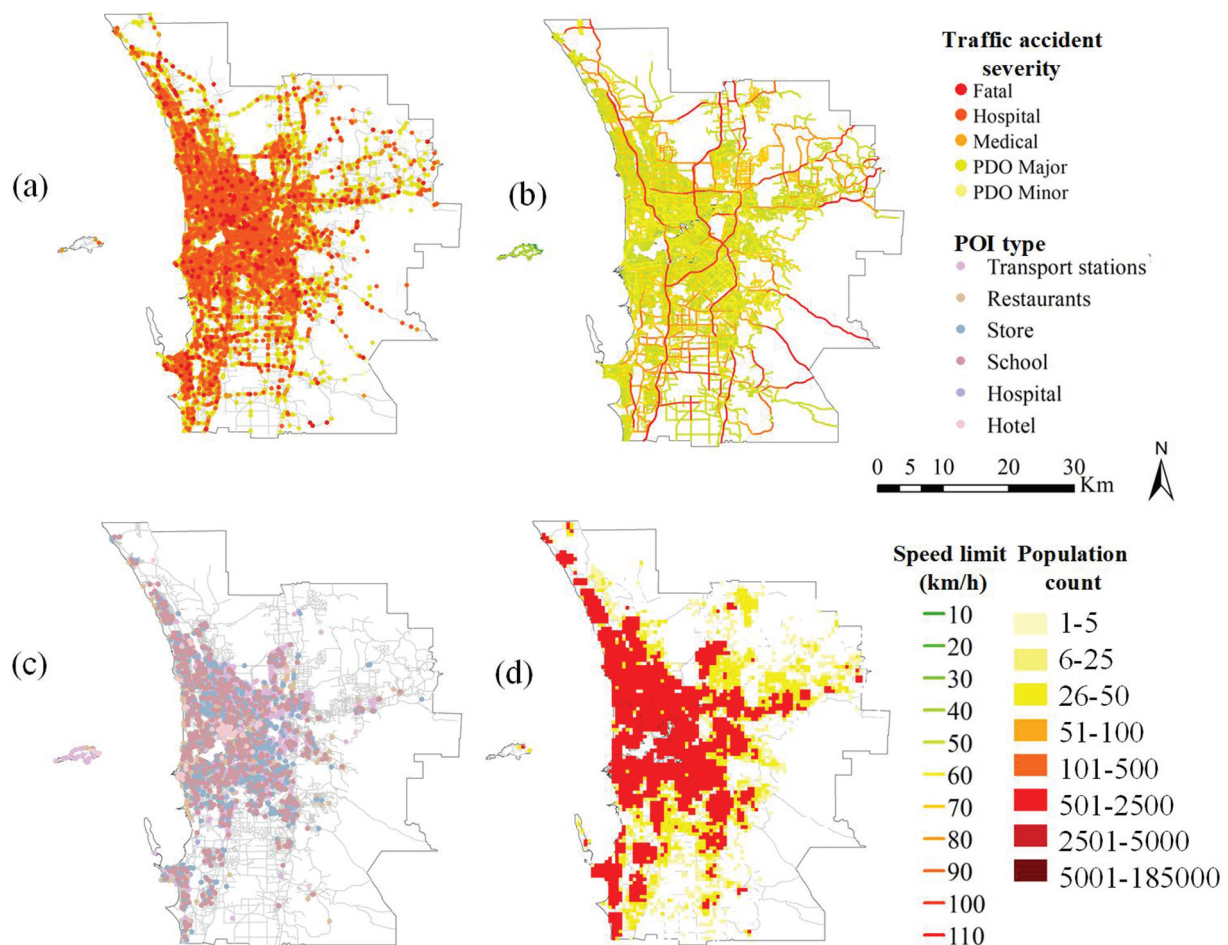


Figure 2. (a) Spatial distribution of traffic accident severity from 2018.1.1 to 2022.12.31 in Perth; (b) spatial distribution of traffic speed limit in Perth; (c) spatial distribution of points of interest (POIs) in Perth; (d) spatial distribution of population density in Perth.

Table 2. Statistics of road speed limit for road segments in Perth.

Speed limit for the road segment (km/h)	Number of road segments under speed limit	Proportion of road segments under speed limit
10	52	0.14%
20	8	0.02%
30	65	0.18%
40	547	1.52%
50	32220	89.55%
60	1219	3.39%
70	1028	2.86%
80	437	1.21%
90	64	0.18%
100	305	0.85%
110	35	0.10%

Table 3. Statistics of POIs types in Perth.

POIs type	Number	Proportion
Transport stations	5654	50.01%
Restaurants	2353	20.81%
Store	1743	15.42%
School	1142	10.10%
Hospital	292	2.58%
Hotel	121	1.08%

risks, with detailed statistics available in Table 3. Figure 2d illustrates the spatial distribution of population density in Perth, indicating that areas with high population density are primarily concentrated in the western city center, with decreasing density toward the outskirts of the city.

Figure 3 depicts the temporal variation of traffic accident severity from 2018.1.1 to 2022.12.31. This

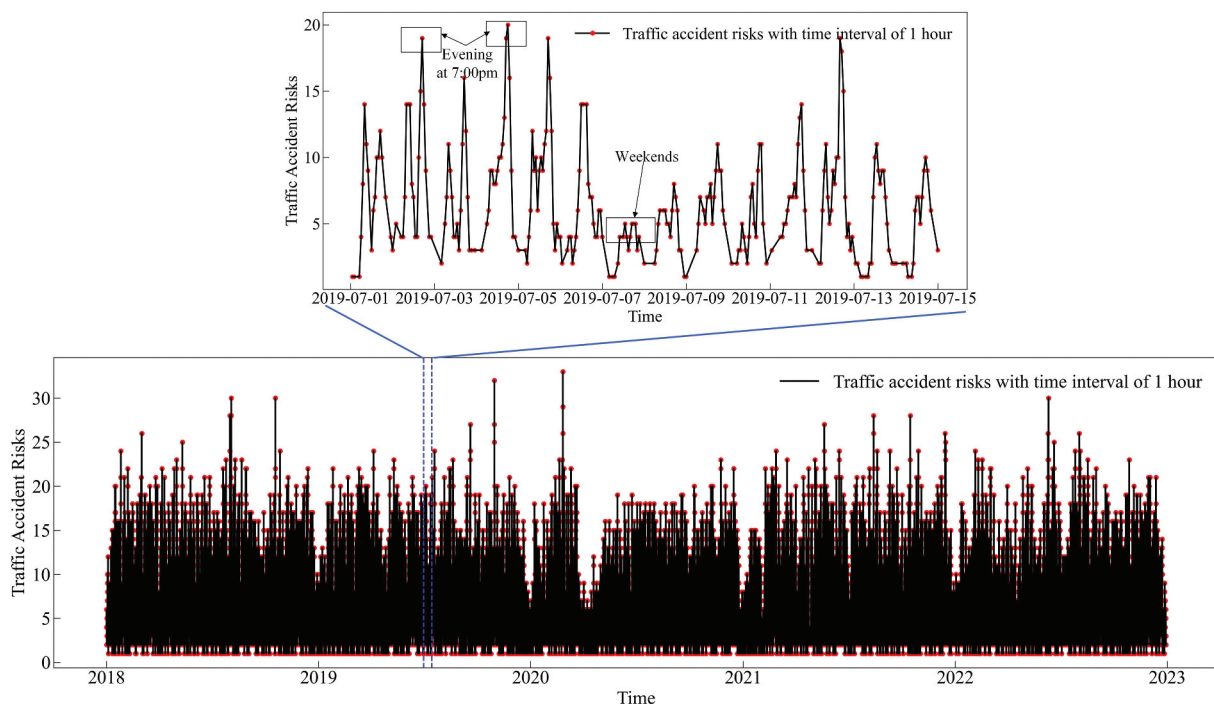
study classified traffic accident types into five categories: minor, major, medical, hospital, and fatal. To quantify these types, we assign numerical values from 1 to 5, respectively, indicating the severity of each accident. We then calculate the traffic accident risk as the weighted sum of the accident types recorded during that period. The data shows a cyclical pattern in traffic accident risks, with the highest incidence usually around 7 PM, attributed to increased vehicle congestion during the evening rush hour. In contrast, the lowest number of accidents is observed on weekends, which may be attributed to reduced traffic volume as fewer individuals commute to work or school.

3. Methodology

Figure 4 illustrates the framework of our study to predict traffic accident risks. It contains several key components, including data collection and processing, constructing a dynamic spatial-temporal deep learning model, model evaluation, and comparison.

3.1. Data collection and processing

The first step is data collection, during which we gathered the following data: traffic accident data, points of interest (POIs), road network information, road speed limit data, population data and weather data.

**Figure 3.** The temporal variation of traffic accident severity in Perth from 2018.1.1 to 2022.12.31.

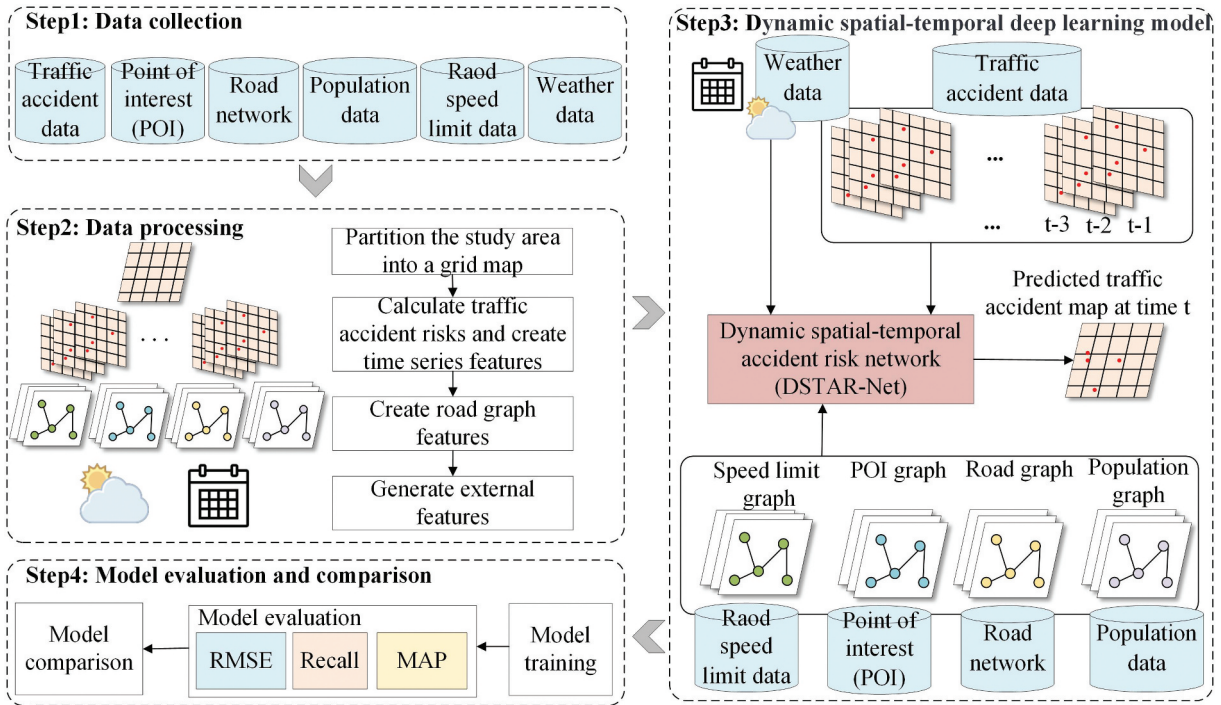


Figure 4. The framework of our study to predict traffic accident risks.

A detailed introduction to this data is provided in the earlier section on the study area and data.

In the data processing phase, we first partition the study area into a uniform grid map of size $H * W$ based on latitude and longitude. This grid structure allows for the effective aggregation of traffic accident information within defined regions.

Following the initial classification of traffic accident types into five categories described in the study area and data section, we calculate the traffic accident risk for each region i within a time interval t as the weighted sum of the accident types recorded during that period.

In addition to these steps, we construct four road feature graphs to describe the similarities among regions in a city from different semantic aspects: the speed limit graph $G_l(V, E_l)$, representing the similarity of speed limits within the region; the road similarity graph $G_s(V, E_s)$, capturing the structural characteristics of road segments, such as the number of road segments and their structures; the POI similarity graph $G_p(V, E_p)$, illustrating the similarity of points of interest (POIs) across regions; and the population graph $G_{pop}(V, E_{pop})$, which represents the population similarities among different areas. Here, G denotes the graph, V is the set of nodes representing different regions, E denotes the set of edges that represent the relationships or similarities

between these nodes, indicating how closely related each node is to one another based on the respective feature being analyzed. The subscripts l, s, p , and pop differentiate the graphs based on the specific feature they represent: speed limits, road structure, points of interest, and population.

Finally, we incorporate external features that influence traffic accidents, such as holidays, weather conditions, and time of day, which we define for each grid as E .

We can formulate the problem based on the above definitions: Let X_t be the grid features of traffic accident risks at the time interval t . M_t are the graph features, including the speed limit graph, road similarity graph, POI similarity graph and population graph at the time interval t . E_t are the external features at time interval t . Our goal is to utilize these historical features to predict a grid map of traffic accident risks for the next hourly interval, $t + 1$, which we denote as Y_{t+1} . Notably, the traffic accident risks are defined as a weighted value derived from both the frequency of accidents and their severity. This model effectively combines various factors related to the roads, population, and historical accident data to forecast the grid-based distribution of traffic accident risks for the upcoming hour.

$$Y_{t+1} = f(X_t, M_t, E_t) \quad (1)$$

3.2. Dynamic spatial-temporal deep learning model

Figure 5 shows the structure of dynamic spatial-temporal accident risk network (DSTAR-Net) for predicting traffic accident risks. It includes spatial-temporal part, semantic part and external part.

3.2.1. Spatial-temporal part

The spatial-temporal part is designed to capture the spatial and temporal dependency between the grids of all regions. This study employed channel-wise CNN to capture the spatial correlation of traffic accidents across geographical regions. Geographically proximate grid cells tend to have similar traffic characteristics and geographical features (Song 2023), thus exhibiting a similar probability of traffic accidents. For example, imagine a city where a major arterial road with poor conditions sees many vehicles passing through on weekends. This arterial road traverses multiple distinct grid cells. In a particular grid cell G1, traffic accidents frequently occur due to poor road conditions. Given the high traffic volume and similar environmental factors, the neighboring grid cell G2 is expected to experience similar traffic accidents.

Most previous research has utilized convolutional neural networks (CNNs) to capture local spatial correlations within a domain (O'Shea 2015; Purwono et al. 2022). Generally, traditional CNN models focus solely on local spatial dimensions (Alzubaidi et al. 2021). Consequently, this study adopts a channel-wise CNN block to account for the effects of various feature characteristics (Han et al. 2020). This block includes the multi-channel CNN and squeeze-and-excitation networks (SENet) (Hu, Shen, and Sun 2018). The formula for the multi-channel CNN is as follows:

$$C^{t,i} = \text{ReLU}(W^{t,i} * X^{t-1,i}) + b^{t,i} \quad (2)$$

where X is the input features, i is the layer of convolution network, $W^{t,i}$ and $b^{t,i}$ are trainable weights; The activation function is *Relu* function; $*$ is the convolution operate.

After I convolutional layers, the output is $C^{t,I} = [c_1, c_2, \dots, c_c]$, where each c_i is a learned feature embedding on each channel. For SENet, the global average pooling is used to generate channel-wise statistic:

$$s = \frac{1}{H * W} \sum_{i=1}^H \sum_{j=1}^W c(i,j) \quad (3)$$

Then we use two fully-connected (FC) layers to learn the nonlinear relationship between different channels:

$$y = \delta(W_2 * \text{ReLU}(W_1 * s)) \quad (4)$$

where W_1 and W_2 are the parameters of FC layers and δ is the sigmoid activation function. Finally, we used the formula to generate the output:

$$F^t = C^{t,i} + y * C^{t,i} \quad (5)$$

Apart from spatial correlations, short-term and long-term temporal correlations can exist between regions. For example, if an accident occurs in a particular area today, the neighboring regions are more prone to similar accidents in the following days or weeks. To capture both long-term and short-term temporal correlations of spatial features across regions, we use time series data F_1, F_2, \dots, F_t from the most recent m time intervals and the previous n weeks as input. We then apply a gated recurrent unit (GRU) to model the temporal traffic-related dependencies (Dey and Salem 2017). The GRU processes these inputs by first computing the update gate z_t using the formula:

$$z_t = \sigma(W_z F_t + U_z h_{t-1} + b_z) \quad (6)$$

where σ is the sigmoid activation function, W_z and U_z are the weight matrices for the input F_t and the previous hidden state h_{t-1} , b_z is the bias term for the update gate.

Next, the reset gate r_t is calculated as:

$$r_t = \sigma(W_r F_t + U_r h_{t-1} + b_r) \quad (7)$$

where W_r and U_r are the weight matrices for the input F_t and the previous hidden state h_{t-1} , b_r is the bias term for the reset gate.

The candidate hidden state $\tilde{h}t$ is then determined by:

$$\tilde{h}t = \tanh(W_h F_t + U_h (r_t \odot ht - 1) + b_h) \quad (8)$$

where \tanh is the hyperbolic tangent activation function, W_h and U_h are the weight matrices for the input F_t and the reset-modified previous hidden state $r_t \odot ht - 1$, b_h is the bias term for the candidate hidden state, \odot denotes element-wise multiplication.

Finally, the hidden state is updated using:

$$h_t = (1 - z_t) \odot h_{t-1} + z_t \odot \tilde{h}t \quad (9)$$

where h_t is the updated hidden state at time.

To improve the model's capability of extracting features from significant time steps, an attention mechanism is incorporated (Vaswani et al. 2017). The attention score e_t is computed as:

$$e_t = \mathbf{w}^T \tanh(\mathbf{W}_h h_t + \mathbf{W}_F F_t) \quad (10)$$

where \mathbf{w} is a learnable parameter vector, \mathbf{W}_h and \mathbf{W}_F are weight matrices for the hidden state h_t and the input feature F_t , respectively.

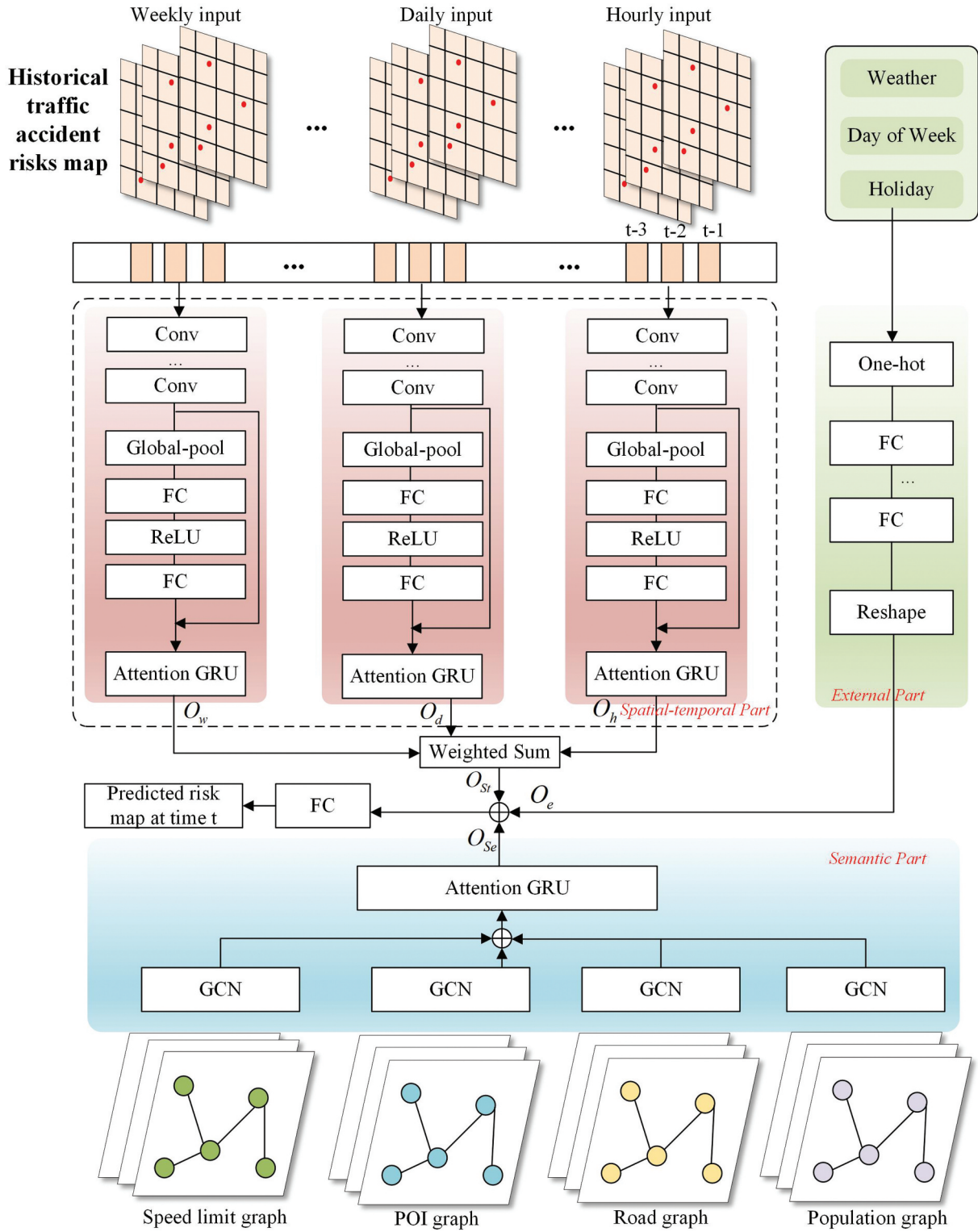


Figure 5. Structure of dynamic spatial-temporal accident risk network (DSTAR-Net) for predicting traffic accident risks.

The attention weights α_t are then derived using the softmax function:

$$\alpha_t = \frac{\exp(e_t)}{\sum_{i=1}^T \exp(e_i)} \quad (11)$$

where α_t is the attention weight for time step t .

Finally, the attention output $\hat{h}t$ is obtained by taking the weighted sum of the hidden states:

$$\hat{h}t = \sum_{i=1}^T \alpha_i h_i \quad (12)$$

where $\hat{h}t$ is the context vector representing the weighted sum of hidden states.

This attention mechanism allows the model to adaptively focus on the time steps in the input sequence that are more important for the final output, thereby improving overall predictive performance.

In our model, traffic accident data is structured into three distinct temporal inputs: weekly, daily, and hourly. Each of these inputs is processed through channel-wise convolutional neural networks (CNNs) and an attention-based GRU to effectively capture the spatial and temporal correlations inherent in the data.

The weekly, daily, and hourly inputs are fed into the channel-wise CNNs, where each temporal segment is analyzed to highlight its unique spatial characteristics. Simultaneously, these inputs are processed by the attention-based GRU, which utilizes the attention mechanism to focus on the most relevant spatial relationships across different regions.

After processing through these networks, the model produces outputs for each temporal module: an hourly output O_h , a daily output O_d , and a weekly output O_w . Finally, we utilize learnable weights to dynamically combine the outputs from the hourly output O_h , the daily output O_d , and the weekly output O_w to obtain the output of the spatial-temporal part O_{st} . O_{st} can be expressed as:

$$O_{st} = W_h * O_h + W_d * O_d + W_w * O_w \quad (13)$$

where W_h , W_d , W_w are the learnable weight matrices corresponding to each of these outputs.

3.2.2. Semantic part

To capture the dependency of semantic features, this study utilizes four graph convolution networks to model four types of graphs: speed limit graph G_l , POI similarity graph G_p , road similarity graph G_s , population graph G_{pop} .

To assess the similarity between various regions, we employ the Jensen-Shannon (JS) divergence to compute distribution similarity (Fuglede and Topsoe 2004). We take the POIs distribution between regions G_i and G_j as an example:

$$JSD(g_i, g_j) = \frac{1}{2} \sum_k \left(\frac{g_i(k) \log 2g_i(k)}{(g_i(k) + g_j(k))} + \frac{g_j(k) \log 2g_j(k)}{(g_i(k) + g_j(k))} \right) \quad (14)$$

$$Sim(i, j) = 1 - JSD(g_i, g_j) \quad (15)$$

where k is the dimension of g_i and g_j . We constructed the adjacent matrix $A = [A_l, A_p, A_s]$. We then use the GCN network to learn the semantic spatial correlations between different regions (Kipf and Welling 2017).

The GCN operation can be formulated as:

$$H^{(l+1)} = \sigma(\hat{D}^{-\frac{1}{2}} \hat{A} \hat{D}^{-\frac{1}{2}} H^{(l)} W^{(l)}) \quad (16)$$

where $\hat{A} = A + I_N$ is the adjacency matrix with added self-connections, \hat{D} is the diagonal degree matrix of \hat{A} , $H^{(l)}$ is the feature matrix at the l -th layer, $W^{(l)}$ is the learnable weight matrix, and σ is the activation function.

To capture temporal correlations, we use a gated recurrent unit (GRU) integrated with an attention mechanism (J. Zhang et al. 2022). The formulas for the attention-based GRU are shown in equation (6) - (12). And we get the output of semantic part O_{se} .

3.2.3. External part

To improve the accuracy of traffic accident risk prediction, we incorporate external factors that influence traffic patterns, focusing on the day of week, holidays, and weather conditions. Recognizing that traffic behavior can fluctuate significantly, we integrate this data information into our model. We utilize a one-hot encoding scheme (Rodríguez et al. 2018), employing an eight-bit format where the first seven bits correspond to the days of the week, and the eighth bit indicates whether it is a weekday or holiday. For example, the encoding $\{1,0,0,0,0,0,1\}$ signifies Monday as a weekday, while $\{0,0,0,0,0,1,0,0\}$ denotes Saturday as a holiday. In addition, we employ two stacked fully connected layers (FC) to process the information. The final output vector is then reshaped and represented as O_e .

3.2.4. Fusion module

Next, we apply weighted fusion to the outputs from the spatial-temporal part O_{st} , the semantic part O_{se} , and the external part O_e to obtain the final prediction O_{t+1} :

$$O_{t+1} = \sigma(W_{st} * O_{st} + W_{se} * O_{se} + W_e * O_e + b) \quad (17)$$

where W_{st} , W_{se} , and W_e are the learnable weight matrices corresponding to the spatial-temporal, semantic, and external part. The term b is a bias added to the final output, and σ represents the activation function, which is a sigmoid function.

The rationale behind this fusion mechanism lies in the varying importance of different spatial-temporal patterns and external factors when predicting traffic accident risk for the next time step. The model can adaptively integrate these heterogeneous features to achieve the most accurate predictions by assigning learnable weights to the outputs from these diverse modules.

The fusion strategy allows the model to learn the optimal way to integrate the complementary information from the hourly, daily, weekly, external, and

semantic parts, using their respective strengths to enhance the overall prediction performance.

To tackle the zero-inflated problem, the model utilizes a weighted loss function, a variation of the mean squared error (MSE) loss (Wang, Lin, et al. 2021). The main concept is to give greater weights to samples with higher cumulative risk scores for traffic accidents during training, preventing the final prediction from having too many zero values.

The loss function is formulated as follows:

$$\text{Loss}(O, \hat{O}) = \frac{1}{2} \sum_{i \in I} \lambda_i (O_{i,t} - \hat{O}_{i,t})^2 \quad (18)$$

where O and \hat{O} represent the ground truth and predicted values, respectively. $I = [0, 1, 2, \geq 3]$ is the set of categories based on the cumulative accident risk score. λ_i is the weight assigned to the i -th accident risk score category.

The weighted loss function aims to prioritize samples with higher cumulative accident risk scores during training. This approach enables the model to improve its predictions for cases with greater accident risk, which is essential for real-world applications.

3.3. Model evaluation

To assess the accuracy of the predicted traffic accident risk, the study utilizes three performance metrics: root mean squared error (RMSE), mean absolute error (MAE), and Recall. RMSE and MAE evaluate the model's predictive performance for continuous values, specifically traffic accident risks, providing a measure of the magnitude of prediction errors. Recall measures the model's effectiveness in identifying high-risk regions by assessing the proportion of actual accident-prone areas that are successfully predicted. This combination of metrics ensures a comprehensive evaluation of the model's performance, highlighting its ability to predict accurately while also identifying critical areas for intervention. These metrics are widely used in many models for traffic accident prediction (Bhardwaj et al. 2023; Wang, Lin, et al. 2021).

The RMSE is calculated as follows:

$$\text{RMSE} = \sqrt{\frac{1}{T} \sum_{t=1}^T (O_t - \hat{O}_t)^2} \quad (19)$$

where O_t is the ground truth value at the time interval t , and \hat{O}_t is the predicted value at the time interval t . RMSE provides a measure of the average magnitude of the errors.

The Recall is computed as:

$$\text{Recall} = \frac{1}{T} \sum_{t=1}^T \frac{|H_t \cap R_t|}{|R_t|} \quad (20)$$

where R_t represents the regions where accidents occur, and H_t denotes the top R_t regions predicted by our model. The intersection of H_t and R_t divided by R_t gives the proportion of high-accident areas identified. Recall assesses the model's capacity to accurately identify these high-risk regions, which is crucial for effectively predicting traffic accident risk. A higher Recall value indicates that the model is successful in recognizing a greater proportion of actual accident locations, thereby supporting timely interventions and enhancing traffic safety measures.

The MAP is defined as:

$$\text{MAP} = \frac{1}{T} \sum_{t=1}^T \frac{\sum_{j=1}^{|R_t|} p_j * r_j}{|R_t|} \quad (21)$$

where p_j indicate the precision of a ranked list from 1 to j . r_j be the recall of region i .

The study evaluates the model's predictive performance by presenting RMSE, Recall, and MAP. RMSE indicates the overall magnitude of errors, while Recall reflects the model's sensitivity to positive instances. MAP improves the evaluation of prediction accuracy. These metrics assess the model's effectiveness in forecasting traffic accident risk in the study area.

4. Experiments and results

4.1. Model settings

In our experiment, we divided the data into three sets: training, validation, and test, following a ratio of 6:2:2. The entire city area is segmented into a grid composed of 20×20 cells Wang, Lin, et al. (2021; Wang, Zhang, et al. 2021). It is important to note that not every region contains a road network; therefore, we retained only those regions with a road network as valid cells for our analysis. As a result, we selected a total of 188 regions for these predictions.

To enhance the effectiveness of our training process, we apply max-min normalization to all data prior to training. Within the graph convolutional network (GCN) framework for each view, we implement two layers of graph convolution operations, each utilizing 64 kernels. We define the convolution kernel size for the channel-wise CNN block module as $3 * 3$. Finally, we set the learning rate to 10^{-4} and the batch size to 32 for our training iterations. The learning curve of DSTAR-Net on Perth dataset, shown in Figure 6, indicates that we employed early stopping to address overfitting.

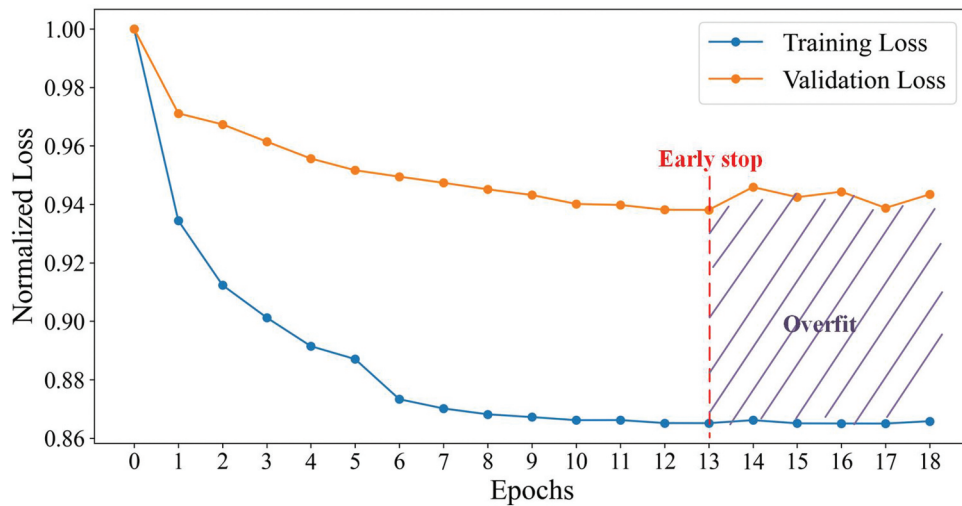


Figure 6. Learning curves of DSTAR-Net on Perth dataset.

Table 4. Comparison of RMSE, Recall and MAP between different models.

Metric	HA	LSTM	ConvLSTM	GSNet	TWCCNet	DSTAR-Net
RMSE	35.641	28.663	27.416	25.601	25.12	24.901
Recall	14.336%	16.56%	18.34%	21.32%	21.33%	21.59%
MAP	0.03825	0.0401	0.06016	0.0623	0.0699	0.0721

4.2. Model evaluation and comparison

To assess the accuracy of our model, we performed a comparative analysis alongside several existing traffic accident prediction models. The baselines against which our model was evaluated include the following:

HA: The historical average (HA) model, a traditional approach in traffic accident prediction, estimates future accident occurrences based on historical data averages.

LSTM (Sutskever 2014): Long short-term memory (LSTM) networks are a well-known deep learning approach for time series forecasting. They excel at capturing nonlinear relationships within temporal data, making them suitable for predicting traffic accident risks.

ConvLSTM (Shi et al. 2015): ConvLSTM integrates convolutional layers with LSTM architecture. This combination allows for convoluted state transitions, enabling effective handling of spatial-temporal data.

GSNet (Wang, Lin, et al. 2021): This recently introduced framework effectively captures intricate spatial-temporal correlations from geographical and semantic perspectives in traffic accident risk prediction.

TWCCNet (Bhardwaj et al. 2023): It is an architecture known as topographic-weighted context category, which modifies the weights of diverse contextual categories according to spatial-temporal correlations in various sectors.

Table 4 compares seven models' RMSE, Recall, and MAP values. DSTAR-Net significantly outperforms existing state-of-the-art models in predicting traffic accident risks, achieving an RMSE of 24.901, a Recall of 21.59%, and a MAP of 0.0721. Following DSTAR-Net, TWCCNet shows the second lowest errors, while GSNet ranks third. In contrast, the HA model exhibits the highest error rates. The superior accuracy of our model results from its effective ability to capture spatial and temporal correlations across different periods and its integration of various data sources, including road features and contextual factors.

4.3. Visualization

Figure 7 shows the performance map of different methods for predicting hourly traffic accident risks. Figures 7a-f display the predicted values for each method, while Figure 7g presents the ground truth. Results show that some traditional methods, such as HA and LSTM, fail to consider spatial factors, resulting in inaccuracies in predicted locations and values. Although CovLSTM considers spatial relationships, it does not consider other influencing factors, leading to predictions that are better than traditional methods but still inaccurate. GSNet and TWCCNet, the latest CNN-GCN methods, can identify the locations and values of accidents with greater accuracy. Our proposed DSTAR-Net method incorporates additional road features and

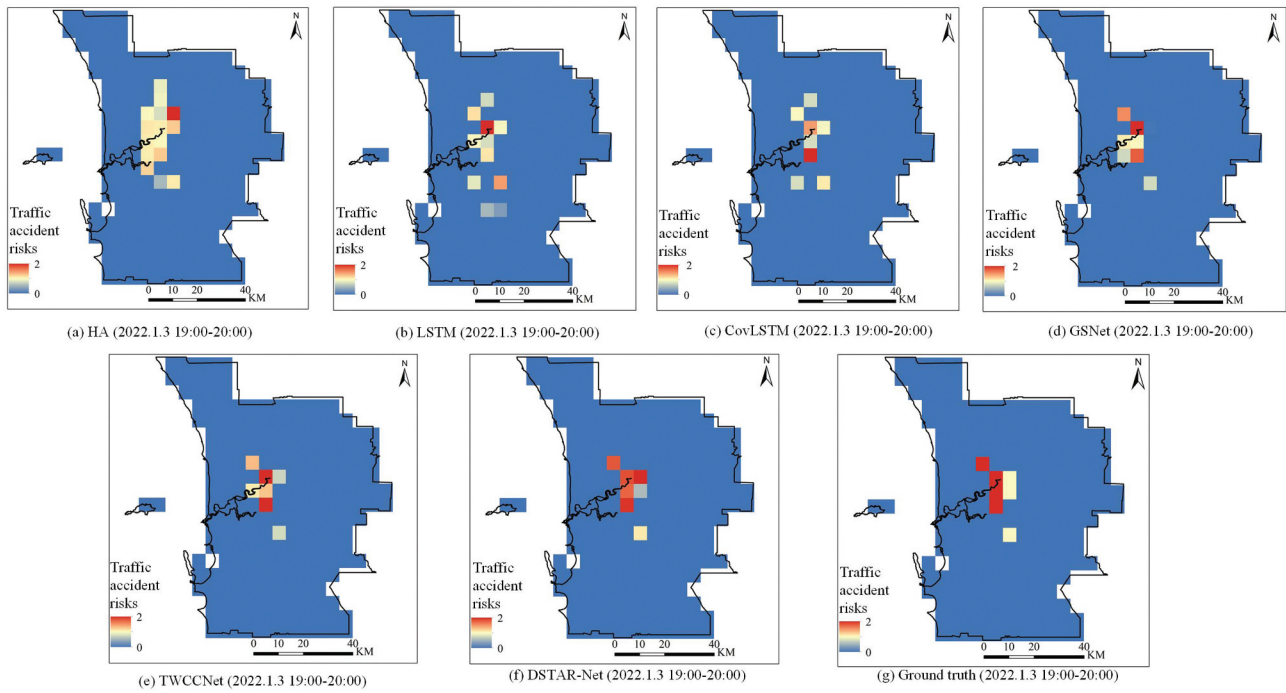


Figure 7. Comparison maps of different methods of traffic accident risks between prediction and ground truth: (a) HA prediction; (b) LSTM prediction; (c) CovLSTM prediction; (d) GNet prediction; (e)twccnet prediction; (f) DSTAR-Net prediction; (g) ground truth.

external factors while also considering the impact of multi-temporal dimensions with different weights, allowing it to make more precise predictions for the spatial locations and values of accidents.

To further analyze our model's prediction results, we examined the spatial distribution of absolute errors (the absolute difference between predicted and ground truth) using the hourly predictions. The results were then aggregated to assess performance at daily and weekly levels. As shown in Figure 8, our model demonstrates better performance in city center areas, primarily

due to the dense road networks, rich road features, and higher frequencies of traffic accidents. Consequently, the model can more effectively capture these complex traffic patterns. In contrast, in the city's edge areas, the model exhibits more significant errors, which may be due to sparse road features, lower traffic volumes, and the randomness of accident occurrences.

Our study explored integrating multi-temporal dimensions into our model. Our results demonstrate that this multi-temporal approach enhances model performance. Specifically, the ablation experiments detailed

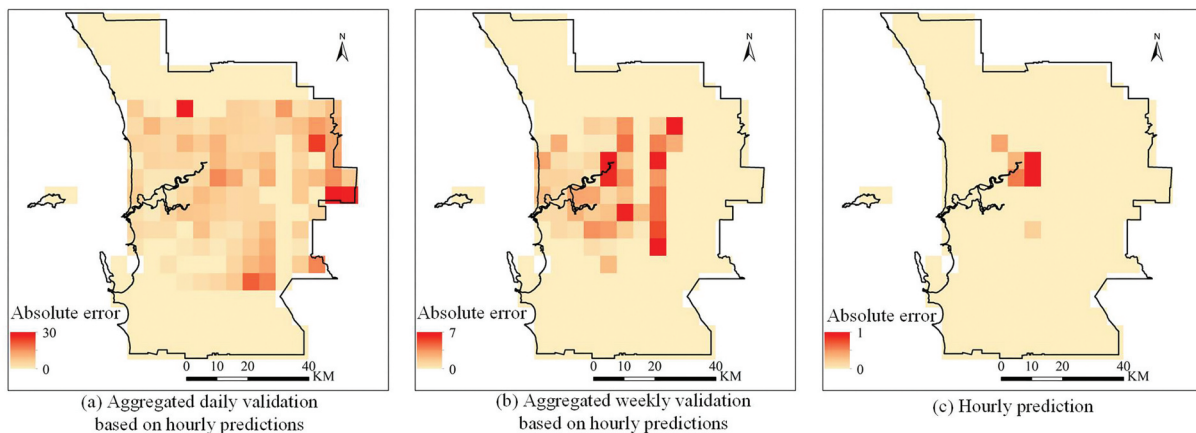


Figure 8. The absolute error distribution maps are presented for (a) aggregated daily validation based on hourly predictions; (b) aggregated weekly validation based on hourly predictions; and (c) hourly prediction.

Table 5. Comparison of the impact of multi-temporal components in DSTAR-Net performance.

Part	RMSE	Recall	MAP
Weekly part only	25.455	21.24%	0.0676
Daily part only	25.314	21.26%	0.0697
Hourly part only	25.241	21.37%	0.0703
Hourly+Daily+Weekly	24.901	21.59%	0.0721

in Table 5 reveal that excluding any single temporal component results in a noticeable increase in RMSE, underscoring the importance of their combined use. When only the weekly, daily, or hourly components are used, the RMSE values are 25.455, 25.314, and 25.241, respectively. In contrast, integrating all three components yields a lower RMSE of 24.901, indicating a performance improvement of approximately 2.2%. These results suggest that the dynamic fusion of these temporal dimensions is crucial for capturing the complex patterns inherent in traffic data.

We also conducted a further analysis comparing the spatial distribution of weights assigned to different inputs of DSTAR-Net. Figure 9 illustrates the weights for the model's (a) weekly input, (b) daily input, and (c) hourly input. The results indicate that the average weight for the hourly input is the highest at 0.390, followed by the daily input at 0.355 and the weekly input at 0.255. These weights, learned through the model, suggest that short-term factors, represented by the hourly component, play a more significant role in influencing traffic accidents than daily and weekly factors.

The lower weights assigned to the daily and weekly components suggest that, although these factors influence overall risk, they are less important for accurate predictions than short-term data. This finding emphasizes the need to prioritize immediate information to capture better the dynamics of rapidly changing road conditions, which can lead to more effective accident prevention strategies. Our analysis shows that while

hourly patterns are most influential due to their ability to capture immediate fluctuations, such as rush hour congestion, including daily and weekly patterns, it is essential for recognizing longer-term trends, such as variations in traffic accidents across different days of the week. This comprehensive approach allows the model to make more accurate predictions using short-term and long-term temporal dynamics.

4.4. Impact of network structure

We also analyzed the impact of network structure. Figure 10 illustrates the component analysis of DSTAR-Net, where we sequentially removed the external part, the semantic part, and the spatial-temporal part. Our findings indicate that removing the spatial-temporal part had the most significant impact, resulting in a 5.6% increase in RMSE.

The increase can be attributed to the role that spatial-temporal features play in predicting traffic accident risks. Without this component, the model struggles to accurately capture the patterns and trends associated with accident occurrences, ultimately degrading its predictive performance.

In Figure 10, we further analyzed other parameters of the model. In Figure 10a, the length of the sequence for hourly input was found to be optimal at 3, indicating that this timeframe effectively captures the relevant trends in traffic data. In Figure 10b, the optimal length for the daily input sequence was found to be 3, as it effectively captures daily fluctuations in accident risks. In Figure 10c, a sequence length of 2 for weekly input proved most effective, as it captures key weekly patterns without unnecessary complexity.

In Figure 10d, the number of GCN filters was optimal at 64, allowing the model to learn complex relationships while avoiding overfitting. In Figure 10e, the learning

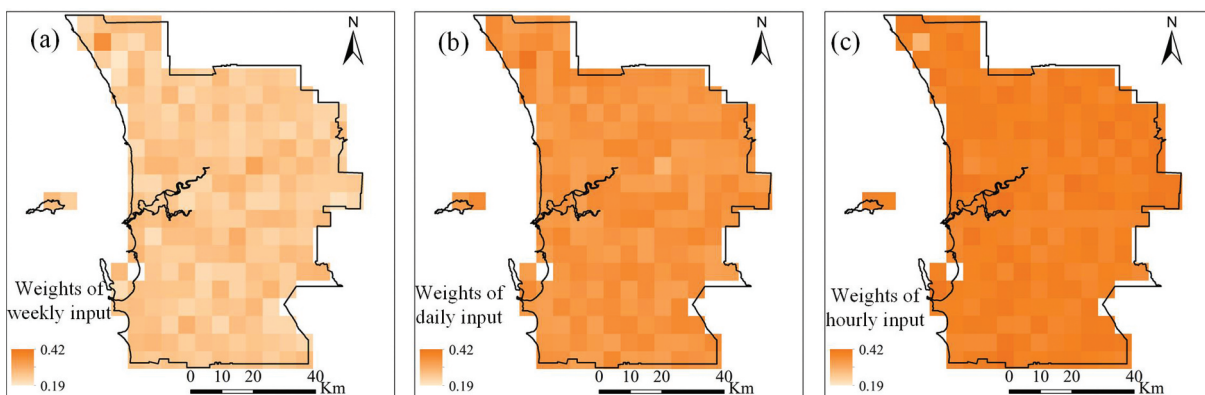


Figure 9. Spatial distribution of weights for different inputs of the DSTAR-Net: (a) weekly input, (b) daily input, (c) hourly input.

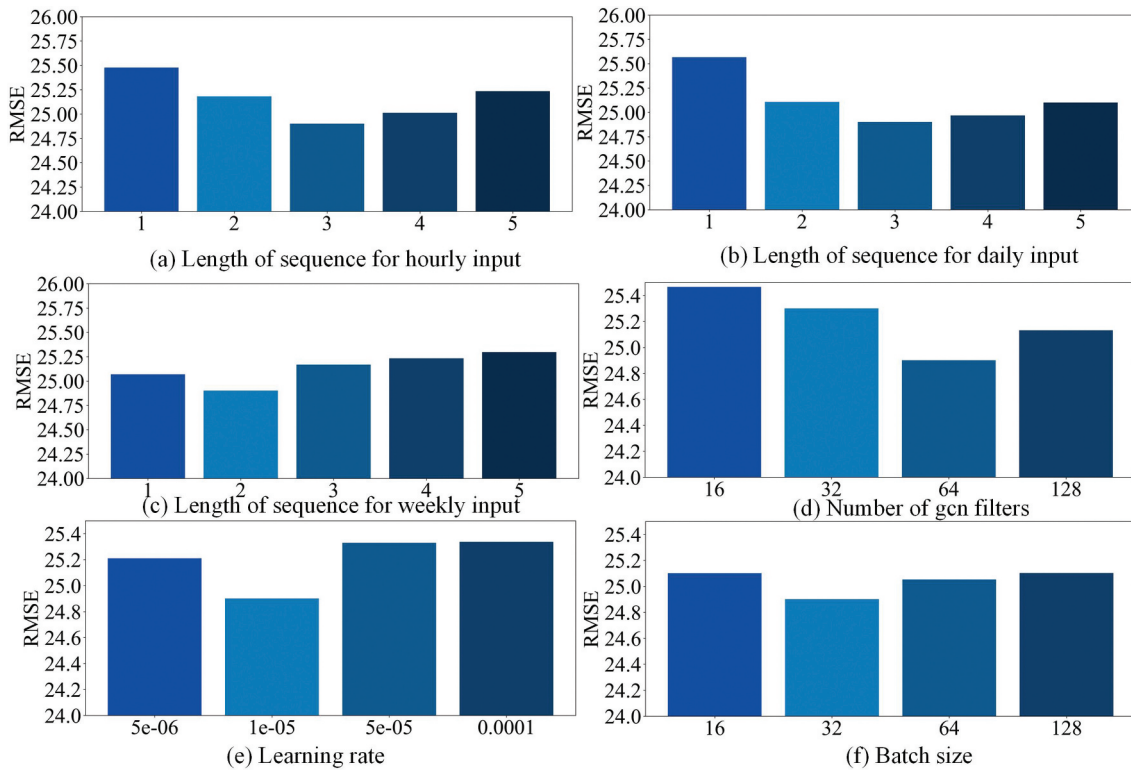


Figure 10. Impact of the network structure: (a) length of sequence for hourly input; (b) length of sequence for daily input; (c) length of sequence for weekly input; (d) number of gcn filters; (e) learning rate; (f) batch size.

rate of 10^{-5} was identified as the most effective, facilitating stable convergence during training. Lastly, in [Figure 10f](#), a batch size of 32 was optimal, balancing computational efficiency with stable gradient updates.

5. Discussion

The findings of this study highlight the effectiveness of the dynamic spatial-temporal accident risk network (DSTAR-Net) in enhancing traffic accident risk predictions in Perth. The model learns the spatial correlations of traffic accidents across weekly, daily, and hourly intervals, effectively capturing the temporal patterns influencing accident occurrences. Combining channel-wise convolutional neural networks (CNNs) with graph convolutional networks (GCNs) enhances the analysis of local geographic dependencies and global semantic relationships. Our model enhances predictive accuracy and enables dynamic adjustments based on contextual factors such as weather and time. The results lead to more relevant and practical information for urban planners and safety officials.

These advances solve two key challenges: handling sparse data through multi-scale analysis, and untangling complex spatial-temporal relationships. Multi-

granularity data analysis is crucial for overcoming issues related to data sparsity and the complexity of spatial-temporal correlations. This innovative approach improves predictive accuracy and reveals the specific factors that affect traffic safety. The methods and findings contribute valuable knowledge to urban computing and traffic management, demonstrating how advanced machine learning techniques can effectively tackle real-world challenges.

To further demonstrate the transferability of our model, we applied DSTAR-Net to the Open New York dataset, which has been widely utilized in prior research (Bhardwaj et al. 2023; Wang, Lin, et al. 2021). By analyzing traffic accident data from 1 January 2013, to 31 December 2013, totaling 147,000 incidents, we compared the performance of our model against existing models using metrics such as RMSE, Recall, and MAP, as shown in [Table 6](#). The results indicate that DSTAR-Net outperforms these models, showcasing its adaptability and robustness across different urban environments. This case study highlights the model's potential for application beyond Perth, reinforcing its relevance for urban planners and safety officials in diverse contexts. Successful implementation in a different dataset emphasizes the model's versatility in addressing traffic accident prediction challenges in various cities. This adaptability

Table 6. Comparison of RMSE, Recall and MAP in open New York dataset.

Metric	HA	LSTM	ConvLSTM	GSNet	TWCCNet	DSTAR-Net
RMSE	10.341	8.723	7.944	7.509	7.251	7.108
Recall	23.95%	28.01%	30.58%	33.68%	34.0%	34.43%
MAP	0.103	0.121	0.151	0.185	0.189	0.192

is crucial for enhancing traffic safety measures and developing effective interventions tailored to specific urban characteristics.

However, the current study does have limitations. One notable concern is the reliance on historical data, which may not adequately account for sudden changes in traffic behavior due to new infrastructure developments or shifts in urban mobility patterns. Future work should add real-time adaptive learning to update models with fresh data, enabling better responses to dynamic conditions. While DSTAR-Net effectively incorporates various contextual factors, exploring the interactions between these factors could further reveal deeper connections related to accidents.

Ultimately, the ongoing development of more robust traffic accident prediction models will facilitate the implementation of effective traffic safety interventions, contributing to the creation of safer urban environments and advancing the field of traffic risk analysis.

6. Conclusion

This study presents the dynamic spatial-temporal accident risk network (DSTAR-Net), a novel framework that significantly enhances the prediction of traffic accident risks in Perth, Western Australia. DSTAR-Net captures complex temporal patterns and integrates multiple data sources, including local geographic and contextual factors. Integrating channel-wise convolutional networks with graph convolutional networks strengthens the analysis of accident risk, resulting in increased predictive accuracy. The findings indicate that DSTAR-Net outperforms current leading methods, providing a powerful tool for traffic risk assessment.

The implications of this research extend beyond Perth, as enhanced traffic accident prediction capabilities can significantly impact city safety and global transportation planning. DSTAR-Net can assist policymakers and urban planners develop targeted interventions to reduce accidents and improve road safety by providing valuable information about traffic patterns and risk factors. Furthermore, the methodologies established in this study can be applied to other urban environments, fostering safer transportation systems worldwide and supporting smart city initiatives. Future research should focus on incorporating adaptive learning mechanisms that enable real-time updates based on new data and

investigate the interactions between various contextual factors to uncover deeper understandings related to traffic accidents.

Disclosure statement

No potential conflict of interest was reported by the author(s).

Funding

This research work was supported by the National Natural Science Foundation of China [Grant Nos. 72201229, 72361137006] and Centre for Infrastructure Delivery Research Funding P0055981.

ORCID

Yongze Song  <http://orcid.org/0000-0003-3420-9622>
Peng Wu  <http://orcid.org/0000-0002-3793-0653>

Data availability statement

The data that support the findings of this study are available at <https://figshare.com/s/b4de470b529f837aa157> <https://figshare.com/s/b4de470b529f837aa157>.

References

- Abdulhafedh, A. 2017. "Road Crash Prediction Models: Different Statistical Modeling Approaches." *Journal of Transportation Technologies* 7 (2): 190–205. <https://doi.org/10.4236/jtts.2017.72014>.
- Ahmed, S. K., M. G. Mohammed, S. O. Abdulqadir, R. G. A. El-Kader, N. A. El-Shall, D. Chandran, M. E. U. Rehman, and K. Dhama. 2023. "Road Traffic Accidental Injuries and Deaths: A Neglected Global Health Issue." *Health Science Reports* 6 (5): e1240. <https://doi.org/10.1002/hsr2.1240>.
- Ali, Y., F. Hussain, and M. M. Haque. 2024. "Advances, Challenges, and Future Research Needs in Machine Learning-Based Crash Prediction Models: A Systematic Review." *Accident Analysis & Prevention* 194:107378. <https://doi.org/10.1016/j.aap.2023.107378>.
- Alkaabi, K. 2023. "Identification of Hotspot Areas for Traffic Accidents and Analyzing Drivers' Behaviors and Road Accidents." *Transportation Research Interdisciplinary Perspectives* 22:100929. <https://doi.org/10.1016/j.trip.2023.100929>.
- Alzubaidi, L., J. Zhang, A. J. Humaidi, A. Al-Dujaili, Y. Duan, O. Al-Shamma, J. Santamara, M. A. Fadhel, M. Al-Amidie, and L. Farhan. 2021. "Review of Deep Learning: Concepts, Cnn Architectures, Challenges, Applications, Future Directions."

- Journal of Big Data* 8 (1): 1–74. <https://doi.org/10.1186/s40537-021-00444-8>.
- Ambros, J., Jurewicz, S., Turner, M., Kieć, J., KieÀ Ambros, C., Jurewicz, and S. Turner. 2018. "An International Review of Challenges and Opportunities in Development and Use of Crash Prediction Models." *European Transport Research Review* 10 (2): 1–10. <https://doi.org/10.1186/s12544-018-0307-7>.
- Anjuman, T., S. Hasanat-E-Rabbi, C. K. A. Siddiqui, and M. M. Hoque. 2020. "Road Traffic Accident: A Leading Cause of the Global Burden of Public Health Injuries and Fatalities." *InProc Int Conf Mech Eng Dhaka Bangladesh*: 29–31.
- Bhardwaj, N., A. Pal, & D. Das. 2023. "Adaptive Context Based Road Accident Risk Prediction Using Spatio-Temporal Deep Learning." *IEEE Transactions on Artificial Intelligence*.
- Bougna, T., G. Hundal, and P. Taniform. 2022. "Quantitative Analysis of the Social Costs of Road Traffic Crashes Literature." *Accident Analysis & Prevention* 165:106282. <https://doi.org/10.1016/j.aap.2021.106282>.
- Brühwiler, L., C. Fu, H. Huang, L. Longhi, and R. Weibel. 2022. "Predicting individuals' Car Accident Risk by Trajectory, Driving Events, and Geographical Context." *Computers, Environment and Urban Systems* 93:101760. <https://doi.org/10.1016/j.compenvurbsys.2022.101760>.
- Bucsuházy, K., E. Matuchová, R. Zúvala, P. Moravcová, M. Kostíková, and R. Mikulec. 2020. "Human Factors Contributing to the Road Traffic Accident Occurrence." *Transportation Research Procedia, Transport Infrastructure and Systems in a Changing world. Towards a more sustainable, reliable and smarter mobility.TIS Roma 2019 Conference Proceedings, Rome, Italy, 555–561, Vol. 45*. <https://www.sciencedirect.com/science/article/pii/S2352146520302192>.
- Chand, A., S. Jayesh, and A. Bhasi. 2021. "Road Traffic Accidents: An Overview of Data Sources, Analysis Techniques and Contributing Factors." *Materials Today: Proceedings* 47, 5135–5141.
- Chen, C., X. Fan, C. Zheng, L. Xiao, M. Cheng, and C. Wang. 2018. "Sdcae: Stack Denoising Convolutional Autoencoder Model for Accident Risk Prediction via Traffic Big Data." *2018 sixth International Conference on Advanced Cloud and Big Data (CBD)*, Lanzhou, China, 328–333. IEEE.
- Chen, F., S. Chen, and X. Ma. 2016. "Crash Frequency Modeling Using Real-Time Environmental and Traffic Data and Unbalanced Panel Data Models." *International Journal of Environmental Research and Public Health* 13 (6): 609. <https://doi.org/10.3390/ijerph13060609>.
- Chen, H., S. Hu, R. Hua, and X. Zhao. 2021. "Improved Naive Bayes Classification Algorithm for Traffic Risk Management." *EURASIP Journal on Advances in Signal Processing* 2021 (1 (1)): 30. <https://doi.org/10.1186/s13634-021-00742-6>.
- Dey, R., and F. M. Salem. 2017. "Gate-Variants of Gated Recurrent Unit (Gru) Neural Networks." *2017 IEEE 60th International midwest Symposium on Circuits and Systems (MWSCAS)*, Boston, MA, USA, 1597–1600. IEEE.
- Fuglede, B., and F. Topsoe. 2004. "Jensen-Shannon Divergence and Hilbert Space Embedding." *International Symposium On Information Theory, 2004. ISIT 2004. Proceedings*, Paderborn, Germany, 31. IEEE.
- Graves, A. 2012. "Long short-Term Memory." *Sequence Labelling with Recurrent Neural Networks*, Vol. 385 of *Studies in Computational Intelligence*, 37–45. Berlin: Springer. https://doi.org/10.1007/978-3-642-24797-2_4.
- Gutierrez-Osorio, C., and C. Pedraza. 2020. "Modern Data Sources and Techniques for Analysis and Forecast of Road Accidents: A Review." *Journal of Traffic & Transportation Engineering (English Edition)* 7 (4): 432–446. <https://doi.org/10.1016/j.jtte.2020.05.002>.
- Han, H.-Y., Y.-C. Chen, P.-Y. Hsiao, and L.-C. Fu. 2020. "Using Channel-Wise Attention for Deep Cnn Based Real-Time Semantic Segmentation with Class-Aware Edge Information." *IEEE Transactions on Intelligent Transportation Systems* 22 (2): 1041–1051. <https://doi.org/10.1109/TITS.2019.2962094>.
- Hossain, M., M. Abdel-Aty, M. A. Quddus, Y. Muromachi, and S. N. Sadeek. 2019. "Real-Time Crash Prediction Models: State-Of-The-Art, Design Pathways and Ubiquitous Requirements." *Accident Analysis & Prevention* 124:66–84. <https://doi.org/10.1016/j.aap.2018.12.022>.
- Hu, J., L. Shen, and G. Sun. 2018. "Squeeze-And-Excitation Networks." *Proceedings of the IEEE Conference on Computer Vision and Pattern Recognition*, Salt Lake City, UT, USA, 7132–7141.
- Jamal, A., M. Zahid, M. Tauhidur Rahman, H. M. Al-Ahmadi, M. Almoshaogeh, D. Farooq, and M. Ahmad. 2021. "Injury Severity Prediction of Traffic Crashes with Ensemble Machine Learning Techniques: A Comparative Study." *International Journal of Injury Control and Safety Promotion* 28 (4): 408–427. <https://doi.org/10.1080/17457300.2021.1928233>.
- Kipf, T. N., and M. Welling. 2017. "Semi-Supervised Classification with Graph Convolutional Networks." *Proceedings of the 5th International Conference on Learning Representations (ICLR 2017)*, 1–14. <https://doi.org/10.48550/arXiv.1609.02907>.
- Lana, I., J. Del Ser, M. Velez, and E. I. Vlahogianni. 2018. "Road Traffic Forecasting: Recent Advances and New Challenges." *IEEE Intelligent Transportation Systems Magazine* 10 (2): 93–109. <https://doi.org/10.1109/IMITS.2018.2806634>.
- Manning, F. 2018. "Temporal Instability and the Analysis of Highway Accident Data." *Analytic Methods in Accident Research* 17:1–13. <https://doi.org/10.1016/j.amar.2017.10.002>.
- Mohammed, A. A., K. Ambak, A. M. Mosa, and D. Syamsunur. 2019. "A Review of the Traffic Accidents and Related Practices Worldwide." *The Open Transportation Journal* 13 (1): 65–83. <https://doi.org/10.2174/1874447801913010065>.
- Moosavi, S., M. H. Samavatian, S. Parthasarathy, R. Teodorescu, and R. Ramnath. 2019. "Accident Risk Prediction Based on Heterogeneous Sparse Data: New Dataset and Insights." *Proceedings of the 27th ACM SIGSPATIAL International Conference on Advances in Geographic Information Systems (SIGSPATIAL '19)*: 33–42. <https://dl.acm.org/doi/10.1145/3347146.3359078>.
- O'Shea, K. 2015. "An Introduction to Convolutional Neural Networks." *arXiv preprint arXiv:1511.08458*.
- Purwono, P., A. Ma'arif, W. Rahmانيar, H. I. K. Fathurrahman, A. Z. K. Frisky, and Q. M. Ul Haq. 2022. "Understanding of Convolutional Neural Network (Cnn): A Review." *International Journal of Robotics and Control Systems* 2 (4): 739–748. <https://doi.org/10.31763/ijrcs.v2i4.888>.
- Ren, H., Y. Song, J. Wang, Y. Hu, and J. Lei. 2018. "A Deep Learning Approach to the Citywide Traffic Accident Risk

- Prediction." *2018 21st International Conference on Intelligent Transportation Systems (ITSC)*, 3346–3351. IEEE.
- Roads Western Australia, M. 2024. "Crash Information (Last 5 Years) [R]. Technical Report TR-2024/07. Perth: Main Roads Western Australia. <https://catalogue.data.wa.gov.au/dataset/mrwa-crash-information-last-5-years->.
- Rodríguez, P., M. A. Bautista, J. Gonzalez, and S. Escalera. 2018. "Beyond One-Hot Encoding: Lower Dimensional Target Embedding." *Image and Vision Computing* 75:21–31. <https://doi.org/10.1016/j.imavis.2018.04.004>.
- Shaik, M. E., M. M. Islam, and Q. S. Hossain. 2021. "A Review on Neural Network Techniques for the Prediction of Road Traffic Accident Severity." *Asian Transport Studies* 7:100040. <https://doi.org/10.1016/j.eastsj.2021.100040>.
- Shi, G., L. Luo, Y. Song, J. Li, and S. Pan. 2024. "Deep Transformer-Based Heterogeneous Spatiotemporal Graph Learning for Geographical Traffic Forecasting." *iScience* 27 (7): 110175. <https://doi.org/10.1016/j.jisci.2024.110175>.
- Shi, X., Z. Chen, H. Wang, D.-Y. Yeung, W.-K. Wong, and W.-C. Woo. 2015. "Convolutional Lstm Network: A Machine Learning Approach for Precipitation Nowcasting." *Advances in Neural Information Processing Systems* 28:802–810. <https://doi.org/10.48550/arXiv.1506.04214>.
- Song, Y. 2023. "Geographically Optimal Similarity." *Mathematical Geosciences* 55 (3): 295–320. <https://doi.org/10.1007/s11004-022-10036-8>.
- Sutskever, I., O. Vinyals, and Q. V. Le. 2014. "Sequence to Sequence Learning with Neural Networks." *Advances in Neural Information Processing Systems* 27:3104–3112.
- Tang, J., L. Zheng, C. Han, W. Yin, Y. Zhang, Y. Zou, and H. Huang. 2020. "Statistical and Machine-Learning Methods for Clearance Time Prediction of Road Incidents: A Methodology Review." *Analytic Methods in Accident Research* 27:100123. <https://doi.org/10.1016/j.amar.2020.100123>.
- Vaswani, A., N. Shazeer, N. Parmar, J. Uszkoreit, L. Jones, A. N. Gomez, L. Kaiser, and I. Polosukhin. 2017. "Attention is All You Need." *Advances in Neural Information Processing Systems* 30:5998–6008.
- Wang, B., Y. Lin, S. Guo, and H. Wan. 2021. "Gsnnet: Learning Spatial-Temporal Correlations from Geographical and Semantic Aspects for Traffic Accident Risk Forecasting." *Proceedings of the AAAI Conference on Artificial Intelligence, Virtual Event* 35, 4402–4409.
- Wang, S., J. Zhang, J. Li, H. Miao, and J. Cao. 2021. "Traffic Accident Risk Prediction via Multi-View Multi-Task Spatio-Temporal Networks." *IEEE Transactions on Knowledge and Data Engineering* 35 (12): 12323–12336. <https://doi.org/10.1109/TKDE.2021.3135621>.
- Zhang, J., Y. Jiang, S. Wu, X. Li, H. Luo, and S. Yin. 2022. "Prediction of Remaining Useful Life Based on Bidirectional Gated Recurrent Unit with Temporal Self-Attention Mechanism." *Reliability Engineering & System Safety* 221:108297. <https://doi.org/10.1016/j.res.2021.108297>.
- Zhang, Z., Z. Li, and Y. Song. 2024. "On Ignoring the Heterogeneity in Spatial Autocorrelation: Consequences and Solutions." *International Journal of Geographical Information Science* 38 (12): 2545–2571. <https://doi.org/10.1080/13658816.2024.2391981>.
- Zheng, Z., Z. Wang, L. Zhu, and H. Jiang. 2020. "Determinants of the Congestion Caused by a Traffic Accident in Urban Road Networks." *Accident Analysis & Prevention* 136:105327. <https://doi.org/10.1016/j.aap.2019.105327>.
- Zhou, L., S. Pan, J. Wang, and A. V. Vasilakos. 2017. "Machine Learning on Big Data: Opportunities and Challenges." *Neurocomputing* 237:350–361. <https://doi.org/10.1016/j.neucom.2017.01.026>.
- Zhou, Z., Y. Wang, X. Xie, L. Chen, and H. Liu. 2020. "Riskoracle: A Minute-Level Citywide Traffic Accident Forecasting Framework." *Proceedings of the AAAI conference on artificial intelligence* 34, 1258–1265.
- Zhou, Z., Y. Wang, X. Xie, L. Chen, and C. Zhu. 2020. "Foresee Urban Sparse Traffic Accidents: A Spatiotemporal Multi-Granularity Perspective." *IEEE Transactions on Knowledge and Data Engineering* 34 (8): 3786–3799. <https://doi.org/10.1109/TKDE.2020.3034312>.